Elliptic gluon generalized transverse-momentum-dependent distribution inside a large nucleus

Jian Zhou

School of physics, Key Laboratory of Particle Physics and Particle Irradiation (MOE), Shandong University, Jinan, Shandong 250100, China

(Received 14 November 2016; published 19 December 2016)

We evaluate the elliptic gluon generalized transverse-momentum-dependent distribution inside a large nucleus using the McLerran-Venugopalan model. We further show that this gluon distribution can be probed through the angular correlation in virtual photon quasielastic scattering on a nucleus.

DOI: 10.1103/PhysRevD.94.114017

I. INTRODUCTION

The quantum phase space distribution of partons inside a nucleon plays a central role in exploring the tomography picture of nucleon. For a fast moving nucleon, a five-dimensional phase space Wigner distribution which carries the complete information on how a single parton is distributed inside a nucleon has been introduced in the literature [1–4]. The Fourier transform of the Wigner distributions referred to as the generalized transverse-momentum-dependent (GTMD) distributions [5] are normally considered as the mother distributions of transverse-momentum-dependent (TMD) distributions and generalized parton distributions (GPDs). So far, the studies of GTMDs mostly focus on the formal theory side, including model calculations [5–11], the analysis of the multipole structure associated with GTMDs [12,13] as well as the investigation of their QCD evolution properties [14]. Perhaps most interestingly, it has been revealed that one of the GTMDs denoted as $F_{1,4}$ [5] can be related to the parton canonical orbital angular momentum [3,15].

Recently, the issue of how to access GTMDs experimentally is attracting growing attentions. In the context of small x formalism, the impact parameter dependent unintegrated gluon distributions often show up in the cross sections of diffractive processes [16–23]. The equivalence of gluon TMDs and small x unintegrated gluon distributions has been first established in Ref. [24], and further clarified in Ref. [25]. The similar analysis were extended to the finite N_c case later [26,27]. Following the similar procedure, one could also identify the impact parameter dependent unintegrated gluon distributions as gluon Wigner distributions due to the same operator structure [28]. Therefore, one is allowed to probe gluon GTMDs in various high energy diffractive scattering processes once a small x factorization framework is employed.

Since the impact parameter $b_\perp$ and the gluon transverse momentum $q_\perp$ are left unintegrated in the current case, one can define a new gluon Wigner distribution, the so-called elliptic gluon Wigner distribution [28] associated with the nontrivial angular correlation $2(q_\perp \cdot b_\perp)^2 - 1$. The integrated version of this gluon distribution is known as the helicity flip gluon GPDs [29,30]. It has been shown that the elliptic gluon distribution naturally emerges after implementing the impact parameter dependent Balistsky-Fadin-Kuraev-Lipatov (BFKL)/Balistsky-Kovchegov (BK) evolution [28,31–36] (for a previous detailed numerical analysis, see Ref. [37]). This finding inspires us to construct a saturation model for the elliptic gluon distribution which can be used as a proper initial condition for the small x evolution. In addition to this motivation, a semiclassical model calculation of the elliptic gluon distribution would be helpful for deepening our understanding of how the tomography picture of nucleon/nucleus is affected by the saturation effect. To be more specific, we will compute the elliptic gluon GTMD in the McLerran-Venugopalan (MV) model [38] that has been widely used to calculate the both unpolarized and polarized small x gluon TMDs [39–43]. In the end, we point out that this gluon distribution is accessible through a $\cos 2\phi$ azimuthal asymmetry in virtual photon-nucleus quasielastic scattering. Such measurement can be performed at the future Electron-Ion-Collinder (EIC).

The rest of the paper is structured as follows. In the next section, we present some details of the evaluation of the gluon elliptic GTMD in the MV model. In Sec. III, we derive the azimuthal dependent cross section for the virtual photon-nucleus quasielastic scattering. The paper is summarized in Sec. IV.

II. THE ELLIPTICAL GLUON GTMD IN THE MV MODEL

As is well known, gluon TMDs are process dependent and correspondingly possess the different gauge link structure. The same statement applies to gluon GTMDs as well. In the present work, we focus on discussing the dipole-type gluon GTMD, which is defined as the following [28,44]:

$$xG_{DP}(x,q_\perp,\Delta_\perp) = 2\int \frac{d\xi^- d^2\xi_\perp e^{-iq_\perp\cdot\xi_\perp - ixP^+\xi^-}}{(2\pi)^3 P^+} \times \left\langle P+\frac{\Delta_\perp}{2}\middle|\mathrm{Tr}[F^{+i}(\xi/2)U^{[-]\dagger}F^{+i}(-\xi/2)U^{[+]}]\middle|P-\frac{\Delta_\perp}{2}\right\rangle, \tag{1}$$

where $\Delta_\perp$ is the transverse momentum transfer to nucleus. Here the longitudinal momentum transfer to nucleus is ignored. The gauge link in the current case takes a closed loop form in the fundamental representation. In the small x limit, up to the leading logarithm accuracy the above expression can be reduced to [28]

$$xG_{DP}(x,q_\perp,\Delta_\perp) = \left(q_\perp^2 - \frac{\Delta_\perp^2}{4}\right)\frac{2N_c}{\alpha_s}\Phi_{DP}(q_\perp,\Delta_\perp) \tag{2}$$

with $\Phi_{DP}(q_\perp,\Delta_\perp)$ being given by

$$\Phi_{DP}(x,q_\perp,\Delta_\perp) = \int\frac{d^2b_\perp d^2r_\perp}{(2\pi)^4}e^{-iq_\perp\cdot r_\perp - i\Delta_\perp\cdot b_\perp}\frac{1}{N_c}\left\langle\mathrm{Tr}\left[U\left(b_\perp+\frac{r_\perp}{2}\right)U^\dagger\left(b_\perp-\frac{r_\perp}{2}\right)\right]\right\rangle. \tag{3}$$

From a phenomenological point of view, the correlation limit where $|\Delta_\perp| \ll |q_\perp|$ is the most interesting kinematical region. In such a kinematical limit, depending on the angular correlation structure, one can parametrize $\Phi_{DP}(x,q_\perp,\Delta_\perp)$ as

$$\Phi_{DP}(x,q_\perp,\Delta_\perp) = \mathcal{F}_x(q_\perp^2,\Delta_\perp^2) + \frac{q_\perp\cdot\Delta_\perp}{|q_\perp||\Delta_\perp|}O_x(q_\perp^2,\Delta_\perp^2) + \left[\frac{(q_\perp\cdot\Delta_\perp)^2}{q_\perp^2\Delta_\perp^2} - \frac{1}{2}\right]\mathcal{F}_x^{\mathcal{E}}(q_\perp^2,\Delta_\perp^2) + \cdots. \tag{4}$$

The Fourier transform of the first term on the right side of the equation $\int d^2\Delta_\perp e^{i\Delta_\perp\cdot b_\perp}\mathcal{F}_x(q_\perp^2,\Delta_\perp^2)$ is the normal impact parameter dependent dipole-type unintegrated gluon distribution. The second term $O_x(q_\perp^2,\Delta_\perp^2)$ is a T-odd (or C-odd) distribution and commonly referred to as the odderon exchange. The expectation value of the spin independent odderon has been computed in a quasiclassical model and shown to be proportional to the slope of the saturation scale [45]. For a transversely polarized target, one can introduce a spin dependent odderon associated with the angular correlation $q_\perp\cdot S_\perp$ where $S_\perp$ is the target transverse spin vector [43,46]. It has been shown in Refs. [47,48] that three different T-odd gluon TMDs can be related to the spin dependent odderon. We refer readers to Ref. [49] for the relevant phenomenology studies of these distributions. The third term, namely the elliptic gluon GTMD $\mathcal{F}_x^{\mathcal{E}}(q_\perp^2,\Delta_\perp^2)$, is what we are interested to compute in the MV model. Higher order harmonics that could exist are not shown in the above equation. Note that the BFKL dynamics only produces even harmonics, while one may expect that odd harmonics could be generated by taking into account the Bartels-Kwiecinski-Praszalowicz (BKP) evolution [50] which describes the asymptotical behavior of the C-odd gluon exchange at high energy.

To gain some intuition how the elliptic gluon distribution emerges from a quasiclassical treatment, it would be instructive to first compute it in the dilute limit. Expanding the Wilson line to the first nontrivial order (neglecting the tadpole type diagram for the moment), one has

$$\Phi_{DP}(x,q_\perp,\Delta_\perp) = \int\frac{d\xi_1^- d\xi_2^- d^2b_\perp d^2r_\perp}{(2\pi)^4}e^{-iq_\perp\cdot r_\perp - i\Delta_\perp\cdot b_\perp}\frac{g_s^2}{2N_c}\left\langle A_a^+\left(\xi_1^-,b_\perp+\frac{r_\perp}{2}\right)A_a^+\left(\xi_2^-,b_\perp-\frac{r_\perp}{2}\right)\right\rangle. \tag{5}$$

Following the standard procedure, we solve the classical Yang-Mills equation and express the gauge field in terms of the color source,

$$A_a^+\left(\xi_1^-,b_\perp+\frac{r_\perp}{2}\right) = \int d^2y_\perp G\left(b_\perp+\frac{r_\perp}{2}-y_\perp\right)\rho_a(\xi_1^-,y_\perp) \tag{6}$$

with

$$G(k_\perp) = \int d^2\xi_\perp e^{-i\xi_\perp\cdot k_\perp} G(\xi_\perp) = \frac{1}{k_\perp^2}. \tag{7}$$

We proceed to evaluate the color source distribution by a Gaussian weight function $W_A[\rho] = \exp[-\frac{1}{2}\int d^3x \frac{\rho_a(x)\rho_a(x)}{\lambda_A(x^-)}]$. This leads to

$$\Phi_{DP}(x, q_\perp, \Delta_\perp) = g_s^2 C_F \int \frac{d^2b_\perp d^2r_\perp d^2x_\perp}{(2\pi)^4} e^{-iq_\perp\cdot r_\perp - i\Delta_\perp\cdot b_\perp} G\left(b_\perp + \frac{r_\perp}{2} - x_\perp\right) G\left(b_\perp - \frac{r_\perp}{2} - x_\perp\right)\mu_A(x_\perp)$$
$$= \frac{g_s^2 C_F}{(2\pi)^4} \frac{1}{(q_\perp - \Delta_\perp/2)^2 (q_\perp + \Delta_\perp/2)^2}\mu_A(\Delta_\perp), \tag{8}$$

where $\mu_A(\Delta_\perp) = \int d^2x_\perp e^{i\Delta_\perp\cdot x_\perp}\mu_A(x_\perp)$ with $\mu_A(x_\perp) = \int d\xi_1^- \lambda_A(\xi_1^-, x_\perp)$. In the correlation limit, we can Taylor expand the above formula in terms of the power $|\Delta_\perp|/|q_\perp|$. According to the parametrization for $\Phi_{DP}(x, q_\perp, \Delta_\perp)$, it is easy to find the following expressions for the gluon GTMDs in the dilute limit:

$$\mathcal{F}_x(q_\perp^2, \Delta_\perp^2) = \frac{\alpha_s C_F}{4\pi^3} \frac{\mu_A(\Delta_\perp)}{q_\perp^4},$$
$$\mathcal{F}_x^{\mathcal{E}}(q_\perp^2, \Delta_\perp^2) = \frac{\Delta_\perp^2}{q_\perp^2}\mathcal{F}_x(q_\perp^2, \Delta_\perp^2). \tag{9}$$

In the below, we will use the above results as the base line to compare with the results in the saturation regime.

To extend the analysis to the saturation regime, we have to take into account all initial/final state interactions encoded in the Wilson lines. We still follow the standard procedure to evaluate the Wilson lines in the MV model. The contributions from the tadpole-type diagram should be included in the current case. The dipole amplitude in the MV model then reads

$$\Phi_{DP}(x, q_\perp, \Delta_\perp) = \int \frac{d^2b_\perp d^2r_\perp}{(2\pi)^4} e^{-iq_\perp\cdot r_\perp - i\Delta_\perp\cdot b_\perp}$$
$$\times e^{-g_s^2 C_F \int d^2x_\perp \mu_A(x_\perp)\left[\frac{G(b_\perp + \frac{r_\perp}{2} - x_\perp)^2}{2} + \frac{G(b_\perp - \frac{r_\perp}{2} - x_\perp)^2}{2} - G(b_\perp + \frac{r_\perp}{2} - x_\perp)G(b_\perp - \frac{r_\perp}{2} - x_\perp)\right]}$$
$$= \int \frac{d^2b_\perp d^2r_\perp}{(2\pi)^4} e^{-iq_\perp\cdot r_\perp - i\Delta_\perp\cdot b_\perp} e^{-\alpha_s C_F \frac{1}{8\pi}\int d^2x_\perp \mu_A(x_\perp)\left[\ln\frac{(b_\perp + \frac{r_\perp}{2} - x_\perp)^2}{(b_\perp - \frac{r_\perp}{2} - x_\perp)^2}\right]^2}. \tag{10}$$

The above expression can be further simplified by making the following approximations valid in the correlation limit. In the perturbative region, the fact that $|r_\perp| \ll |b_\perp| \sim |x_\perp|$ allows us to Taylor expand the logarithm term,

$$\int d^2x_\perp \mu_A(x_\perp)\left[\ln\frac{(b_\perp + \frac{r_\perp}{2} - x_\perp)^2}{(b_\perp - \frac{r_\perp}{2} - x_\perp)^2}\right]^2 \approx \int_{r_\perp}^{1/\Lambda_{\rm QCD}} d^2y_\perp \left\{\frac{4r_\perp^2\cos^2(\phi)}{y_\perp^2} + \frac{2[4\cos^4(\phi) - 3\cos^2(\phi)]r_\perp^4}{3y_\perp^4}\right\}\mu_A(b_\perp - y_\perp), \tag{11}$$

where ϕ is the azimuthal angle between $r_\perp$ and $y_\perp \equiv b_\perp - x_\perp$. Since the integration is dominated by the small $y_\perp$ region, one can make a Taylor expansion in terms of $y_\perp$,

$$\mu_A(b_\perp - y_\perp) \approx \mu_A(b_\perp) - \frac{\partial\mu_A(b_\perp)}{\partial b_\perp^i} y_\perp^i + \frac{1}{2}\frac{\partial^2\mu_A(b_\perp)}{\partial b_\perp^i \partial b_\perp^j} y_\perp^i y_\perp^j. \tag{12}$$

Inserting it into Eq. (11), we obtain

$$\int d^2x_\perp \mu_A(x_\perp)\left[\ln\frac{(b_\perp + \frac{r_\perp}{2} - x_\perp)^2}{(b_\perp - \frac{r_\perp}{2} - x_\perp)^2}\right]^2 \approx 2\pi r_\perp^2 \ln\frac{1}{r_\perp^2\Lambda_{\rm QCD}^2}\mu_A(b_\perp)$$
$$+ \frac{\pi r_\perp^2}{24}\ln\frac{1}{r_\perp^2\Lambda_{\rm QCD}^2}\left\{2\left(r_\perp\cdot\frac{\partial}{\partial b_\perp}\right)^2 - r_\perp^2\frac{\partial}{\partial b_\perp}\cdot\frac{\partial}{\partial b_\perp}\right\}\mu_A(b_\perp). \tag{13}$$

The simple power counting tells us that the second term scales as $\Delta_\perp^2 Q_s^2/q_\perp^4$. In the kinematical region where $Q_s|\Delta_\perp| \ll q_\perp^2$, it is not necessary to sum the second term into the exponential form. Based on this observation, the dipole distribution can be expressed as

$$\Phi_{DP}(x, q_\perp, \Delta_\perp) = \int \frac{d^2 b_\perp d^2 r_\perp}{(2\pi)^4} e^{-iq_\perp \cdot r_\perp - i\Delta_\perp \cdot b_\perp} \times \left[1 - \frac{r_\perp^2}{192}\left\{2\left(r_\perp \cdot \frac{\partial}{\partial b_\perp}\right)^2 - r_\perp^2 \frac{\partial}{\partial b_\perp} \cdot \frac{\partial}{\partial b_\perp}\right\} Q_s^2(b_\perp)\right] e^{-\frac{r_\perp^2 Q_s^2(b_\perp)}{4}}, \quad (14)$$

where $Q_s(b_\perp)$ is the commonly defined impact parameter dependent saturation scale. After carrying out the azimuthal angle integration, one arrives at

$$\mathcal{F}_{x_g}(q_\perp^2, \Delta_\perp^2) = \int \frac{d^2 b_\perp d^2 r_\perp}{(2\pi)^4} e^{-iq_\perp \cdot r_\perp - i\Delta_\perp \cdot b_\perp} \exp\left[-\frac{r_\perp^2 Q_s^2}{4}\right], \quad (15)$$

$$\mathcal{F}_{x_g}^{\mathcal{E}}(q_\perp^2, \Delta_\perp^2) = -\int \frac{d|b_\perp| d|r_\perp|}{(2\pi)^2} J_2(|q_\perp||r_\perp|) J_2(|\Delta_\perp||b_\perp|) \frac{|r_\perp|^5 |b_\perp|^3}{24} \frac{\partial^2 Q_s^2(b_\perp^2)}{\partial^2 b_\perp^2} \exp\left[-\frac{r_\perp^2 Q_s^2}{4}\right], \quad (16)$$

where J_2 is the second order Bessel function. These are the main results of our paper. In the dilute limit where $q_\perp^2 \gg Q_s^2 \gg \Delta_\perp^2$, one can reproduce Eq. (9) by expanding the exponential and keeping the first nontrivial term. This provides us a nice consistency check. Another observation one can make is that the elliptic gluon distribution vanishes if color source were uniformly distributed in the transverse plane of a nucleus. Following the same method, one could also compute the Weizsäcker-Williams (WW) type gluon elliptic GTMD in the MV model. However, we leave it for the future study as it is less interesting phenomenologically [28].

Let us now close this section by presenting a simple numerical estimation. It is rather common to parametrize the $b_\perp$ dependence of the saturation scale as the following [20,23]:

$$Q_s^2 = Q_{s0}^2 \exp\left[-\frac{b_\perp^2}{Bg}\right] \ln\left[\frac{1}{r_\perp^2 \Lambda_{\mathrm{QCD}}^2} + E\right]. \quad (17)$$

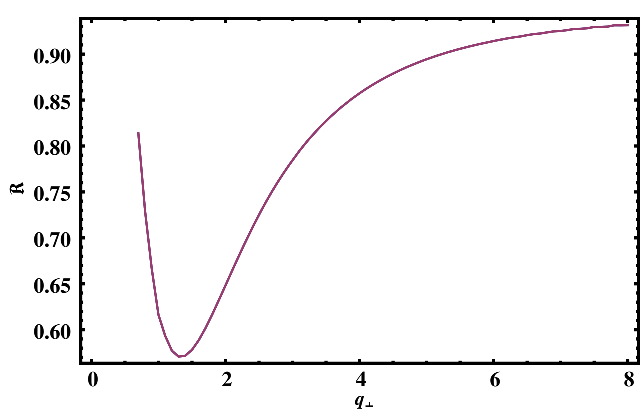

FIG. 1. The double ration $\mathcal{R}$ as the function of $q_\perp$ for $\Delta_\perp = 0.1$ GeV.

We fix the parameters to be $\Lambda_{\mathrm{QCD}} = 0.2$ GeV, $B_g = 8\ \mathrm{GeV}^{-2}$ and $Q_{s0}^2 = 1\ \mathrm{GeV}^2$. Inserting the above formula into Eq. (16), the elliptical gluon distribution takes the form

$$\mathcal{F}_{x_g}^{\mathcal{E}}(q_\perp^2, \Delta_\perp^2) = -\int \frac{d|b_\perp| d|r_\perp|}{(2\pi)^2} J_2(|q_\perp||r_\perp|) J_2(|\Delta_\perp||b_\perp|) \times \frac{|r_\perp|^5 |b_\perp|^3 Q_s^2}{24 B_g^2} \exp\left[-\frac{r_\perp^2 Q_s^2}{4}\right]. \quad (18)$$

We are interested in studying how the elliptic gluon distribution is affected by the saturation effect. To this end, we plot the double ratio defined in the following as the function of $q_\perp$:

$$\mathcal{R}(q_\perp^2, \Delta_\perp^2) = \frac{\mathcal{F}_{x_g}^{\mathcal{E}}/\mathcal{F}_{x_g}}{\Delta_\perp^2/q_\perp^2}, \quad (19)$$

where $\Delta_\perp^2/q_\perp^2$ is the ratio between the elliptic gluon distribution and the normal dipole gluon distribution in the dilute limit. When performing the numerical calculation, we impose a cut off 7 GeV^{-1} for the upper limit of $|b_\perp|$ integration. This effectively corresponds to removing the forward scattering contribution. Our numerical result presented in Fig. 1 indicates that the elliptic gluon distribution is suppressed in the saturation regime, while at high transverse momentum, the double ratio approaches one as expected. We plan to carry out a more detailed numerical analysis in a future publication.

III. OBSERVABLE

In Ref. [28], it has been proposed to probe the elliptic gluon GTMD by measuring diffractive dijet production in electron-nucleus collisions. Such a process was first studied in Ref. [51]. In the back-to-back kinematical limit where the individual jet transverse momentum $P_\perp$ is much larger than the nucleon recoiled momentum $\Delta_\perp$, a $\cos 2(\phi_{P_\perp} - \phi_{\Delta_\perp})$ angular modulation of the cross section of this process is sensitive to the elliptic gluon GTMD. Instead of the diffractive dijet production in eA collisions, we now consider transversely polarized virtual photon-nucleus quasielastic scattering $\gamma^*(q) + A(P) \to A(P') + X$, which also offers us the opportunity to probe the elliptic gluon distribution via the angular correlation $\cos 2(\phi_{\epsilon_T^{\gamma^*}} - \phi_{\Delta_\perp})$, where $\epsilon_T^{\gamma^*}$ is the virtual photon transverse polarization vector.

In the dipole approach, the diffractive cross section for a transversely polarized virtual photon scattering off nucleus has been computed in Refs. [17,18] and takes the form

$$\frac{d\sigma_T}{d^2\Delta_\perp} = \pi \int \frac{dz}{z(1-z)} \int d^2 r_\perp |\Psi_T^{\gamma^*}(Q^2, r_\perp, z)|^2 \times \left\{ \int \frac{d^2 b_\perp}{(2\pi)^2} e^{-ib_\perp \cdot \Delta_\perp} \left[1 - \left\langle \frac{1}{N_c} \mathrm{Tr}\left[U\left(b_\perp + \frac{r_\perp}{2}\right) U^\dagger\left(b_\perp - \frac{r_\perp}{2}\right)\right]\right\rangle \right] \right\}^2, \tag{20}$$

where $\Psi_T^{\gamma^*}(Q^2, r_\perp, z)$ is the transversely polarized virtual photon wave function. The wave function squared can be expressed as

$$|\Psi_T^{\gamma^*}(Q^2, r_\perp, z)|^2 = 2N_c \sum_q \frac{\alpha_{\mathrm{em}} e_q^2}{\pi} z(1-z) \frac{(1-2z)^2 (\epsilon_T^{\gamma^*} \cdot r_\perp)^2 + (\epsilon_T^{\gamma^*} \times r_\perp)^2}{r_\perp^2} \epsilon_f^2 [K_1(|r_\perp| e_f)]^2, \tag{21}$$

where $e_f^2 = Q^2 z(1-z)$ and z is the longitudinal momentum fraction of virtual photon carried by quark. Here, quark mass is ignored. Inserting the MV model results, the azimuthal independent cross section is expressed as

$$\frac{d\sigma_T}{d^2\Delta_\perp} = \pi \int \frac{dz}{z(1-z)} \int d^2 r_\perp \Phi(Q^2, r_\perp^2, z) \left\{ \int \frac{d^2 b_\perp}{(2\pi)^2} e^{-ib_\perp \cdot \Delta_\perp} \left(1 - e^{-\frac{r_\perp^2 Q_s^2}{4}}\right) \right\}^2 \tag{22}$$

while the azimuthal dependent cross section reads

$$\frac{d\sigma_T}{d^2\Delta_\perp}\Big|_{\cos 2\phi} = \frac{2(\epsilon_T^{\gamma^*} \cdot \Delta_\perp)^2 - \Delta_\perp^2}{24 \Delta_\perp^2} \pi \int \frac{dz}{z(1-z)} \int d|r_\perp| \Phi^{\mathcal{E}}(Q^2, r_\perp^2, z) |r_\perp|^5 \times \int d|b_\perp| J_2(|\Delta_\perp||b_\perp|) |b_\perp|^3 \frac{\partial^2 Q_s^2(b_\perp^2)}{\partial^2 b_\perp^2} e^{-\frac{r_\perp^2 Q_s^2(b_\perp^2)}{4}} \int \frac{d^2 b'_\perp}{(2\pi)^2} \left(1 - e^{-\frac{r_\perp^2 Q_s^2(b_\perp'^2)}{4}}\right) \tag{23}$$

with the scalar part of the wave function being given by

$$\Phi(Q^2, r_\perp^2, z) = 2N_c \sum_q \frac{\alpha_{\mathrm{em}} e_q^2}{\pi} z(1-z)[z^2 + (1-z)^2] \epsilon_f^2 [K_1(|r_\perp| e_f)]^2, \tag{24}$$

$$\Phi^{\mathcal{E}}(Q^2, r_\perp^2, z) = 2N_c \sum_q \frac{\alpha_{\mathrm{em}} e_q^2}{\pi} z(1-z)[2z^2 - 2z] \epsilon_f^2 [K_1(|r_\perp| e_f)]^2. \tag{25}$$

If the virtual photon is induced by a lepton, only the V_4 component [52,53] of the corresponding leptonic tensor contributes to the azimuthal dependent cross section. To be precise, the contribution from this component yields a $\cos 2\phi_{e-A}$ azimuthal modulation where ϕ_{e-A} is the angle between the hadron/nucleus plane and the lepton plane. One notices that the azimuthal asymmetry in this process offers us a direct access to the second derivative of the saturation scale with respect to $b_\perp^2$. As such, the elliptic gluon GTMD can be easily determined through measuring this observable.

IV. SUMMARY

We derived the elliptic gluon GTMD inside a large nucleus using the MV model. Our result can be used as the initial condition when implementing small x evolution. We further proposed to probe the elliptic gluon GTMD through the angular correlation in quasielastic virtual photon scattering off a nucleus. This measurement can, in principle, be carried out at the future EIC. Since such a study will deepen our understanding of how the gluon tomography is induced by small x dynamics, it might be worthwhile to pursue a comprehensive numerical analysis of this observable for the typical EIC accessible kinematical region in a future publication.

ACKNOWLEDGMENTS

I would like to thank D. Mueller for bringing to my attention the small x gluon helicity flip GPDs, and Y. J. Zhou for her help with making the plot. This work has been supported by the National Science Foundations of China under Grant No. 11160005131608, and by the Thousand Talents Plan for Young Professionals.

[1] X. d. Ji, Viewing the Proton through, Color, Filters, Phys. Rev. Lett. **91**, 062001 (2003).
[2] A. V. Belitsky, X. d. Ji, and F. Yuan, Quark imaging in the proton via quantum phase space distributions, Phys. Rev. D **69**, 074014 (2004).
[3] C. Lorce and B. Pasquini, Quark Wigner distributions and orbital angular momentum, Phys. Rev. D **84**, 014015 (2011).
[4] C. Lorce, B. Pasquini, X. Xiong, and F. Yuan, The quark orbital angular momentum from Wigner distributions and light-cone wave functions, Phys. Rev. D **85**, 114006 (2012).
[5] S. Meissner, A. Metz, and M. Schlegel, Generalized parton correlation functions for a spin-1/2 hadron, J. High Energy Phys. 08 (2009) 056.
[6] A. Mukherjee, S. Nair, and V. K. Ojha, Quark Wigner distributions and orbital angular momentum in light-front dressed quark model, Phys. Rev. D **90**, 014024 (2014).
[7] A. Courtoy, G. R. Goldstein, J. O. Gonzalez Hernandez, S. Liuti, and A. Rajan, On the observability of the quark orbital angular momentum distribution, Phys. Lett. B **731**, 141 (2014).
[8] K. Kanazawa, C. Lorce, A. Metz, B. Pasquini, and M. Schlegel, Twist-2 generalized transverse-momentum dependent parton distributions and the spin/orbital structure of the nucleon, Phys. Rev. D **90**, 014028 (2014).
[9] T. Liu and B. Q. Ma, Quark Wigner distributions in a light-cone spectator model, Phys. Rev. D **91**, 034019 (2015).
[10] A. Mukherjee, S. Nair, and V. K. Ojha, Wigner distributions for gluons in a light-front dressed quark model, Phys. Rev. D **91**, 054018 (2015).
[11] D. Chakrabarti, T. Maji, C. Mondal, and A. Mukherjee, Wigner distributions and orbital angular momentum of a proton, Eur. Phys. J. C **76**, 409 (2016).
[12] C. Lorce and B. Pasquini, Structure analysis of the generalized correlator of quark and gluon for a spin-1/2 target, J. High Energy Phys. 09 (2013) 138.
[13] C. Lorce and B. Pasquini, Multipole decomposition of the nucleon transverse phase space, Phys. Rev. D **93**, 034040 (2016).
[14] M. G. Echevarria, A. Idilbi, K. Kanazawa, C. Lorce A. Metz, B. Pasquini, and M. Schlegel, Proper definition and evolution of generalized transverse momentum dependent distributions, Phys. Lett. B **759**, 336 (2016).
[15] Y. Hatta, Notes on the orbital angular momentum of quarks in the nucleon, Phys. Lett. B **708**, 186 (2012).
[16] S. J. Brodsky, L. Frankfurt, J. F. Gunion, A. H. Mueller, and M. Strikman, Diffractive leptoproduction of vector mesons in QCD, Phys. Rev. D **50**, 3134 (1994).
[17] W. Buchmuller, T. Gehrmann, and A. Hebecker, Inclusive and diffractive structure functions at small x, Nucl. Phys. **B537**, 477 (1999).
[18] Y. V. Kovchegov and L. D. McLerran, Diffractive structure function in a quasiclassical approximation, Phys. Rev. D **60**, 054025 (1999); Erratum, Phys. Rev. D **62**, 019901(E) (2000).
[19] A. D. Martin, M. G. Ryskin, and T. Teubner, Q^2 dependence of diffractive vector meson electroproduction, Phys. Rev. D **62**, 014022 (2000).
[20] H. Kowalski and D. Teaney, An impact parameter dipole saturation model, Phys. Rev. D **68**, 114005 (2003).
[21] C. Marquet, R. B. Peschanski, and G. Soyez, Exclusive vector meson production at HERA from QCD with saturation, Phys. Rev. D **76**, 034011 (2007).
[22] T. Lappi and H. Mantysaari, Incoherent diffractive J/Psi-production in high energy nuclear DIS, Phys. Rev. C **83**, 065202 (2011).
[23] A. H. Rezaeian, M. Siddikov, M. Van de Klundert, and R. Venugopalan, Analysis of combined HERA data in the impact-parameter dependent saturation model, Phys. Rev. D **87**, 034002 (2013).
[24] F. Dominguez, C. Marquet, B. W. Xiao, and F. Yuan, Universality of unintegrated gluon distributions at small x, Phys. Rev. D **83**, 105005 (2011).
[25] J. Zhou, The evolution of the small x gluon TMD, J. High Energy Phys. 06 (2016) 151.
[26] E. Akcakaya, A. Schäfer, and J. Zhou, Azimuthal asymmetries for quark pair production in pA collisions, Phys. Rev. D **87**, 054010 (2013).
[27] C. Marquet, E. Petreska, and C. Roiesnel, Transverse-momentum-dependent gluon distributions from JIMWLK evolution, J. High Energy Phys. 10 (2016) 065.
[28] Y. Hatta, B. W. Xiao, and F. Yuan, Probing the Small-x Gluon Tomography in Correlated Hard Diffractive Dijet Production in Deep Inelastic Scattering, Phys. Rev. Lett. **116**, 202301 (2016).
[29] P. Hoodbhoy and X. D. Ji, Helicity flip off forward parton distributions of the nucleon, Phys. Rev. D **58**, 054006 (1998).

[30] A. V. Belitsky and D. Mueller, Off forward gluonometry, Phys. Lett. B **486**, 369 (2000).
[31] L. N. Lipatov, The bare pomeron in quantum chromodynamics, Zh. Eksp. Teor. Fiz. **90**, 1536 (1986) [Sov. Phys. JETP **63**, 904 (1986)].
[32] H. Navelet and S. Wallon, Onium-onium scattering at fixed impact parameter: Exact equivalence between the color dipole model and the BFKL pomeron, Nucl. Phys. **B522**, 237 (1998).
[33] H. Navelet and R. B. Peschanski, Conformal invariance and the exact solution of BFKL equations, Nucl. Phys. **B507**, 353 (1997).
[34] K. J. Golec-Biernat and A. M. Stasto, On solutions of the Balitsky-Kovchegov equation with impact parameter, Nucl. Phys. **B668**, 345 (2003).
[35] C. Marquet and G. Soyez, The Balitsky-Kovchegov equation in full momentum space, Nucl. Phys. **A760**, 208 (2005).
[36] B. Z. Kopeliovich, H. J. Pirner, A. H. Rezaeian, and I. Schmidt, Azimuthal anisotropy of direct photons, Phys. Rev. D **77**, 034011 (2008).
[37] Y. Hagiwara, Y. Hatta, and T. Ueda, Wigner, Husimi and GTMD distributions in the color glass condensate, Phys. Rev. D **94**, 094036 (2016).
[38] L. D. McLerran and R. Venugopalan, Gluon distribution functions for very large nuclei at small transverse momentum, Phys. Rev. D **49**, 3352 (1994); Computing quark and gluon distribution functions for very large nuclei, Phys. Rev. D **49**, 2233 (1994).
[39] Y. V. Kovchegov, Non-Abelian Weizsacker-Williams field and a two-dimensional effective color charge density for a very large nucleus, Phys. Rev. D **54**, 5463 (1996).
[40] J. Jalilian-Marian, A. Kovner, L. D. McLerran, and H. Weigert, Intrinsic glue distribution at very small x, Phys. Rev. D **55**, 5414 (1997).
[41] A. Metz and J. Zhou, Distribution of linearly polarized gluons inside a large nucleus, Phys. Rev. D **84**, 051503 (2011).
[42] A. Dumitru, T. Lappi, and V. Skokov, Distribution of Linearly Polarized Gluons and Elliptic Azimuthal Anisotropy in Deep Inelastic Scattering Dijet Production at High Energy, Phys. Rev. Lett. **115**, 252301 (2015).
[43] J. Zhou, Transverse single spin asymmetries at small x and the anomalous magnetic moment, Phys. Rev. D **89**, 074050 (2014).
[44] P. J. Mulders and J. Rodrigues, Transverse momentum dependence in gluon distribution and fragmentation functions, Phys. Rev. D **63**, 094021 (2001).
[45] Y. V. Kovchegov and M. D. Sievert, A new mechanism for generating a single transverse spin asymmetry, Phys. Rev. D **86**, 034028 (2012); Erratum, Phys. Rev. D **86**, 079906(E) (2012).
[46] L. Szymanowski and J. Zhou, The spin dependent odderon in the diquark model, Phys. Lett. B **760**, 249 (2016).
[47] D. Boer, M. G. Echevarria, P. Mulders, and J. Zhou, Single Spin Asymmetries from a Single Wilson Loop, Phys. Rev. Lett. **116**, 122001 (2016).
[48] D. Boer, S. Cotogno, T. van Daal, P. J. Mulders, A. Signori, and Y. J. Zhou, Gluon and Wilson loop TMDs for hadrons of spin ≤ 1, J. High Energy Phys. 10 (2016) 013.
[49] D. Boer, P. J. Mulders, C. Pisano, and J. Zhou, Asymmetries in heavy quark pair and dijet production at an EIC, J. High Energy Phys. 08 (2016) 001.
[50] J. Bartels, High-energy behavior in a non-Abelian gauge theory (II): First corrections to $T_{n\to m}$ beyond the leading $\ln s$ approximation, Nucl. Phys. **B175**, 365 (1980); J. Kwiecinski and M. Praszalowicz, Three gluon integral equation and odd c singlet Regge singularities in QCD, Phys. Lett. **B94**, 413 (1980).
[51] T. Altinoluk, N. Armesto, G. Beuf, and A. H. Rezaeian, Diffractive dijet production in deep inelastic scattering and photon-hadron collisions in the color glass condensate, Phys. Lett. B **758**, 373 (2016).
[52] R. b. Meng, F. I. Olness, and D. E. Soper, Semi-inclusive deeply inelastic scattering at electron-proton colliders, Nucl. Phys. **B371**, 79 (1992).
[53] J. Zhou, F. Yuan, and Z. T. Liang, Hyperon polarization in unpolarized scattering processes, Phys. Rev. D **78**, 114008 (2008).